J Appl Electrochem (2009) 39:2239–2249
DOI 10.1007/s10800-009-9831-4

ORIGINAL PAPER

Electrochemical oxidation process for water condensates recycling in a shuttle orbiter

L. Rutigliano · D. Fino · G. Saracco · V. Specchia · P. Spinelli · L. Grizzaffi

Received: 14 October 2008 / Accepted: 4 February 2009 / Published online: 24 February 2009

Abstract A pilot plant has been built for the regeneration of humidity condensates during shuttle missions. The plant is an automated experimental apparatus which includes an electrochemical cell, two reservoirs and a control system to maintain the temperature within a chosen range, so that the ionic exchange membranes are not damaged. The electrodes used to determine catalytic efficiency were: platinised titanium with ruthenium oxide and Sb and Sn coatings deposited on a Ti substrate, prepared with two different techniques, spray/brush coating and electro-deposition. The $Ti/SnO_2–Sb_2O_5$ coating was characterized through the following techniques: X-ray diffraction (XRD), scanning electron microscopy (SEM), energy dispersion spectroscopy (EDS) and linear and cyclic voltammetry (CV). Among the different contaminant dissolved in the contaminant solution, urea was chosen to carry out the electrochemical tests. Several regenerative treatment runs were performed with the solution simulating the shuttle condensate water to determine the evolution, during the tests, of the total organic carbon (TOC) concentration, the nitrate and nitrite concentrations, the ammonia concentration, the pH and the conductivity. These runs were carried out at different current intensities to understand the influence of the anodic current on the organic decomposition rates, in particular of the urea in presence of an amount of sodium chloride. The contaminant removal efficiencies in the electro-oxidation test appeared to be depressed for both electrodes at high current density, whereas the inversion of the electrode polarity seemed to offer a further advantage. The best result reached in the direct electro-oxidation was the 24 ppm as TOC with $Ti/SnO_2–Sb_2O_5$ at 0.2 A. This value is far from the limit concentration (0.5 ppm), which is the standard level for drinking water in space appliances. During the tests, a decrease in the pH was observed, due to the formation of refractory substances such as organic acids.

Keywords Advanced oxidation process · Electrochemical oxidation · Humidity condensates · $Ti/SnO_2–Sb_2O_5$ electrode · Urea

L. Rutigliano · D. Fino (✉) · G. Saracco · V. Specchia · P. Spinelli
Department of Materials Science and Chemical Engineering, Politecnico di Torino, Corso Duca degli Abruzzi 24, 10129 Turin, Italy
e-mail: debora.fino@polito.it

L. Grizzaffi
Thales Alenia Space Torino-Italia, Strada Antica di Collegno 253, 10146 Turin, Italy

1 Introduction

The supply of water is currently one of the most critical issues on the Earth, as a consequence of serious problems due to desertification of large areas, demographic increases and water contamination.

In very specific and limited conditions, the problem of fresh water supply is also very important for long-term manned missions aimed at exploring the solar system.

Several projects have been proposed in the last years for regenerative support systems concerning atmospheric revitalization, thermal and humidity control, and water reclamation [1, 2]. During manned space missions the accumulated hygiene and condensate water must be reclaimed on board a spacecraft, otherwise the high purity water produced by the fuel cell (as a valuable by-product) during the electrical energy generation is not sufficient to maintain the water balance [3]. Nowadays, the energy

needed to support long-term or permanently manned International Space Station (ISS) missions is provided by solar panel arrays, which exploit the high intensity of UV irradiation. Regenerative processes are therefore required to recycle the cabin air and, in particular, to recover wastewater. Water is produced aboard the shuttle orbiter from different sources: hygiene water, urine, and humidity condensates [4–10]. Several methods currently exist to regenerate wastewater; some of these process the streams separately, whereas other ones treat the water as a single system, combining humidity condensate, hygiene water, and distillate urine in a single wastewater stream to reclaim water, in order to satisfy drinking standards. Aboard the Russian Mir space station, the liquid streams are treated separately and drinking water is produced from humidity condensate since this source has lowest dissolved contaminant level [11]. The humidity condensates are recovered by a cabin air humidity and temperature control system, which has the purpose of maintaining healthy environmental conditions for the crew.

This air stream is cooled in a condensing heat exchanger and the recovered water is stored in a suitable reservoir. The main contaminants are short chain alcohols, carboxylic acids, nitrogen organic compounds and other hydrophilic low molecular weight organics which originate as airborne contaminants due to human metabolism and material outgassing from wet phases aboard [1]. The concentration of contaminants is about 96 ppm as TOC; NASA instead requires a concentration limit of 0.5 ppm, which is much more restrictive compared to the standard level for drinking water. Many techniques have been used to remove contaminants from humidity condensates such as biological treatment, catalytic oxidation, multifiltration or combined treatments [10, 12]. All regenerative processes need to minimize the consumption of reagents and the generation of by-products in order to be compatible with the limited availability of space. An oxidation technique that seems to satisfy all these requirements is electro-oxidation, because it mainly employs electric energy, which may be generated by photovoltaic panels, and uses very small amounts of consumables.

The aim of the present study regards the design, assembly and testing of an electrochemical cell, where electrolytic solutions and humidity condensate are continually circulated by means of a centrifugal pump. The efficiency of the organic electro-oxidation to a great extent depends on the properties of the anodes.

The electrodes used for oxidation of the organic pollutants require high oxygen over-potential to produce a high concentration of the hydroxyl radical, which is the most important oxidant agent generated by an electrochemical process. Highly reactive hydroxyl radicals, generated under oxygen evolution conditions, can either adsorb onto the electrode or generate new oxides when higher oxidation states are available for metal ions in the anodic layer. Adsorbed $OH^{\bullet}$ reacts with organic molecules till complete oxidation to carbon dioxide and water, while higher oxides allow a partial oxidation. Both reactions can be important from the environmental point of view: the reaction between contaminants and the oxide film to a higher oxidation state can improve the yield and selectivity, the other oxidation mechanism allows the complete abatement of pollutants [13, 14].

Other important anode characteristics are high chemical and electrochemical stability together with electrical conductivity. All these features depend on the nature and concentration of the dopant and on the thermal conditions of the treatment. This is in fact found in the case of SnO_2 electrodes doped with Sb, which provide very good efficiency for the disposal of organic pollutants [15, 16]. Another parameter that greatly affects the electrode characteristics, particularly their stability, is the preparation of the substrate.

In this work an SnO_2–Sb_2O_5 coating applied to Ti anodes with the brush technique was prepared and characterized. Over the last 20 years, this type of electrode has been studied in depth for the complete or partial oxidation of organic pollutants in wastewater [17–21]. Tests for the abatement of organic compounds, dissolved in humidity condensates, have been carried with this electrode and the obtained results were compared with those attained with a commercial electrode consisting of titanium platinised with RuO_2.

The tests were performed in a new electrochemical set-up, which allowed many operating parameters, such as pH, TOC, concentration of ammonium nitrate, of ammonia, etc., to be determined and controlled.

2 Experimental section

2.1 Electrode preparation

Pure titanium foil was used as the substrate (150 × 150 × 2 mm, 99.7% purity, Aldrich). The electrode preparation involved several steps: its surface was polished with WS-FLEX 18-C sandpaper (to increase the adhesion between the Ti substrate and the catalytic oxide film, in order to increase the roughness), degreased in 40% NaOH at 80 °C for 2 h, etched in hydrochloric acid 11.5 M for about 60 s, washed in distilled water, dried in air and then treated in an ultrasonic bath at 60 °C for 30 min [22–25]. Following the preliminary treatments, the coating was deposited on the electrode surface by the brush coating method [26].

The deposition on the electrode surface was carried out as follows:

(a) a solution of 20% w/v $SnCl_4 \cdot 5H_2O$ and 0.2% w/v $SbCl_3$ in 2-propanol was spread on the titanium surface using a soft hair paintbrush. The solvent was evaporated at 90 °C for 10 min.
(b) after two applications of the solution, the sample was heated in 0.21 NL min^{-1} oxygen flow at 500 °C for 20 min.
(c) steps (a) and (b) were repeated (12 or 24 times) until the two desired thicknesses of the SnO_2 coating were reached. The average coating thickness was evaluated from the increase in metal sheet weight after deposition, assuming a layer density of about 7 g cm^{-3} [27]. The weight increase was proportional to the number of applications: a 8 g m^{-2} weight gain and about a 1.14 μm average thickness for 12 applications and a 18 g m^{-2} weight gain and about 2.57 μm average thickness for 24 applications.
(d) once the desired thickness had been reached, the samples were subjected to an annealing process at 500 °C for 60 min.

As an alternative to the previous coating procedure, direct electro-deposition was tried out on the Ti substrate, with Sn^{2+} and Sb^{3+} in acid solutions, which were cathodically deposited. Preliminary tests with this technique did not provide satisfactory results, due to the difficulty of finding stable electrical conditions for the electro-deposition.

2.2 Physical and electrochemical properties

The coating morphology and microstructure were examined by X-ray diffraction (PW 1710 Philips Diffractometer) and field emission scanning electron microscopy FESEM; the surface composition of the coating was analyzed using an energy dispersion spectrometer (SEM/EDS LEO 50/50 VP with a Gelmini column).

The cyclic voltammetry and linear anodic voltammetry conducted to determine the electrochemical behaviour were performed with VoltaLab PGZ 301 (Radiometer Copenhagen) instrumentation. Electrochemical tests were carried out in a 0.5 M Na_2SO_4 solution using a Pt foil as the counter-electrode and a Hg/Hg_2SO_4/sat. K_2SO_4 reference electrode (0.64 V vs. SHE) with a Luggin capillary.

2.3 Experimental apparatus

An automated experimental apparatus was designed for the present investigation. Figure 1 shows the electrochemical cell, which was made in perspex to provide the necessary electrical insulation. The cell, working in batch mode with recycling, had two anodic compartments at the two end sections, which increased the surface available for oxidation of the contaminants, and a central chamber acting as the cathodic compartment.

$Ti/SnO_2–Sb_2O_5$ electrode synthesized in our laboratories and the commercial Pt–Ru mixed oxide one deposited on titanium (DSA® electrode from DeNora, Italy) were used as anodes; the cathode was in stainless steel. All the electrodes were of 150 × 150 mm in size.

The cathode was separated from the two anodes by a cationic exchange membrane (CMB Neosepta membrane, Tokuyama Soda Co.). Moreover, turbulence promoter was installed on the anodic electrode surfaces to favour mass transfer. The electrolyte solution (Na_2SO_4 0.01 M) and the condensate water were introduced into the cathodic and into the anodic compartments, respectively.

Both solutions were stored in separated reservoirs and circulated through the electrolytic cell by means of centrifugal pumps. Throttling valves were employed to control

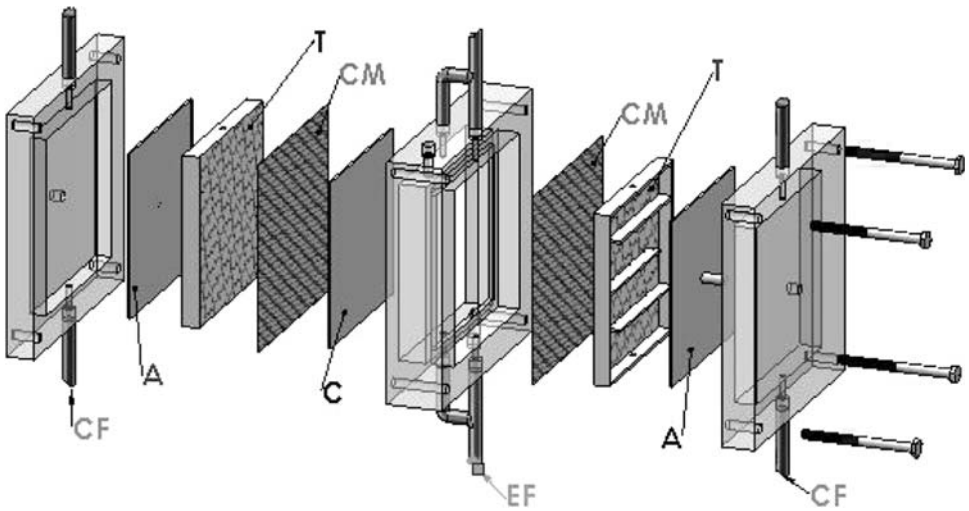

Fig. 1 Exploded cell scheme. *CF* Condensate feed, *A* Anode, *T* turbulence promoter, *CM* Cationic membrane, *C* cathode, *EF* electrolytic feed

the solution flows. The electrochemical tests were carried out under galvanostatic conditions with a current density of between 0.4 and 18 mA cm^{-2}. The reservoirs contained a cooling coil which was necessary to stabilize the temperature of the solutions in the 25–40 °C range. The system was completely automated through the use of a thermocouple (PT 100) connected to a thermo-regulator that simultaneously opened the electro-valve and started the pump, thus allowing the circulation of the cooling water. Important parameters, such as ORP, pH, and conductivity, which are useful to investigate the electrochemical process, were continuously measured.

Chemical analysis was carried out by periodically sampling 10 mL of the anodic solutions and using standard methods for the determination of the nitrogen distribution in the oxidation products. The nitrate concentrations were analyzed through reduction and diazotization, whilst the nitrite concentrations were analyzed by means of the iodometric method. The Nessler method was employed to determine of the ammonia concentration. The combined, free and total chlorine were measured using the *N*,*N*′-diethyl-*p*-phenylenediamine (DPD) standard method by spectroscopic detection. All the chemical species of interest dissolved in the anodic solution were determined through colorimetric determination using the Orbeco-Hellige water analysis system (model 975-MP). TOC determination was obtained from the difference between the TC and TIC with a DR 5000 Hach-Lange spectrophotometer. TC was determined by means of oxidation of the organic carbon with persulphate and evolution of CO_2; TIC was instead determined through acidification.

2.4 Electrolyte solution and water condensates composition

The composition of the solution that the simulates the shuttle condensate water is reported in Table 1.

Table 1 Main contaminants present in the humidity water aboard the ISS

Contaminants	TOC (ppm)	N total (ppm)	Cl total (ppm)
Carboxylic acids	18	–	–
Alcohols	60	–	–
Ketones, aldehydes	7	–	–
Nitrogen organic compounds	11.2	11	–
Ammonium ions	–	17.5	–
Nitrate ions	–	0.5	–
Chloride salts	–	–	6

3 Results

3.1 Structure tests

The XRD patterns of the Ti/SnO_2–Sb_2O_5 electrode prepared by brush coating with 12 (A) and 24 (B) applications of metal solution on a Ti surface, show peaks that indicate the crystalline structure of SnO_2, a mixed Sn and Sb oxide; whereas with 12 depositions instead a Ti peak is present that points out an incomplete uniform deposition on the electrode surface. When the electrode was prepared with 24 layers, a decreasing in half-width of the peaks was observed, consequently a better crystallinity of SnO_2 and $Sn_{0.918}$ $Sb_{0.109}$ O_2 was obtained, probably due to the previous oxide depositions, which provided very good adhesion of the subsequent coatings.

The SEM images of the Ti/SnO_2–Sb_2O_5 electrodes prepared by brush coating showed more homogeneous structure for the 24 layer deposition, than that of the other one, which presented larger grains, as a consequence of a lower number of fractures, and therefore of a lower specific surface and a decrease of film resistivity.

Cracked and shadow zones (attributable to TiO_2) were observed on the electrode with 12 depositions; the formation of TiO_2, characterized by poor conductivity, caused the SnO_2–Sb_2O_5 film to fail and the catalytic activity to decline [28, 29].

3.2 Electrochemical testing

Anodic linear sweep voltammetry was carried out at a low potential scan rate of 10 mV/s to determine the value of oxygen over-potential. Figure 2 shows that the marked current increase attributed to oxygen evolution was reached at about 1.35 V vs. Hg/Hg_2SO_4. Considering that the pH of the test solution is close to neutrality, the oxygen overpotential is about 1.2 V. This provides interesting conditions

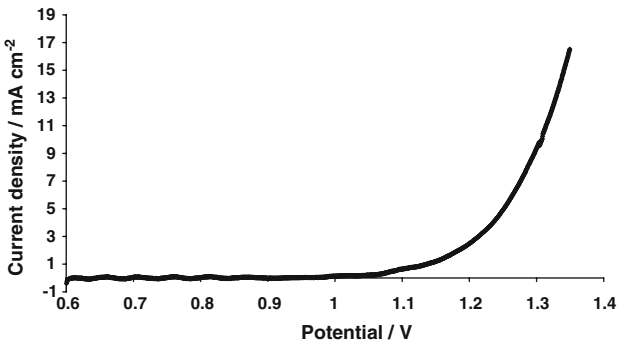

Fig. 2 Density current variation in neutral solution (Na_2SO_4 0.5 M electrolyte) during potential scanning at 10 mV s^{-1} over a SnO_2/Sb_2O_5 on Ti. Reference electrode: Hg/Hg_2SO_4

for anodic oxidation of dissolved species. The semi-logarithmic plot of the voltammetry of Fig. 2, after the ohmic drop correction, allowed the Tafel slope for oxygen evolution, which was equal to 0.157 V dec^{-1}, to be determined**.** This value is rather high, but not unusual for highly oxidizing electrodes [30]. However, the discussion of this point is beyond the scope of the present work. The high over-potential value suggests the formation of hydroxyl radicals, which are known to effectively participate into the direct electro-oxidation of organic pollutants.

An example of the electrochemical characterization of the oxidizing conditions in the presence of urea was obtained by performing some cyclic voltammetry tests with SnO_2–Sb_2O_5 as the working electrode, a Pt counter electrode and a Hg/Hg_2SO_4 reference electrode. The electrolyte was a 0.5 M Na_2SO_4 solution. Cyclic voltammetry was carried out both in the absence and in the presence of urea, which was added to the electrolyte in an amount of 0.7 g/L. The potential scan rate was 100 mV/s. The potential scan was started in the proximity of the open circuit potential.

Figure 3 compares the first cycle of such CV tests in the presence and in the absence of urea. It can be noted that the open circuit potential when urea is present is markedly lowered from about 0.3 to 0.1 V vs. Hg/Hg_2SO_4. This is clear evidence of the strong adsorption of urea on the electrode surface. The anodic branch of the voltammetry does not present an anodic peak for urea oxidation, thus indicating that such a process occurs in the region of oxygen evolution, and involves OH radicals (below 1.84 V vs. SHE) [31].

A closer look at such behaviour is reported in Fig. 4, which only shows the anodic branch of the CV tests. The curves in the upper graph illustrate the differences during

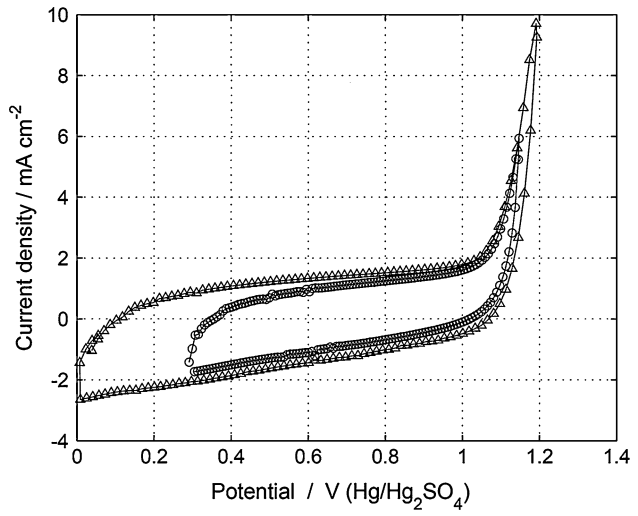

Fig. 3 Cyclic voltammetry at 100 mV s^{-1} of SnO_2/Sb_2O_5 on Ti without urea (*open circle*) and with urea (0.7 g L^{-1}) plus electrolyte (0.5 M Na_2SO_4) (*open triangle*). Reference electrode: Hg/Hg_2SO_4

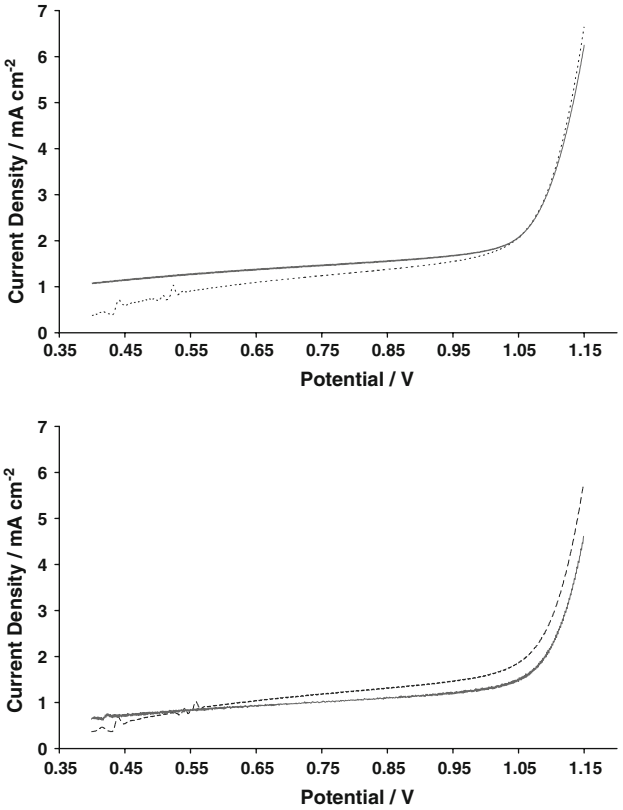

Fig. 4 Enlargement of oxidation zone of the cyclic voltammetry at 100 mV s^{-1} of SnO_2/Sb_2O_5 on Ti without urea (dashed line) and with urea (0.7 g L^{-1}) plus electrolyte (0.5 M Na_2SO_4) (continuous line); first cycle (upper graph), fourth cycle (lower graph). Reference electrode: Hg/Hg_2SO_4

the first cycle with and without urea, while the lower graph refers to the fourth cycle. It can be observed that, during the first cycle, the anodic current in the presence of urea is higher than that found without urea up to the potential for oxygen evolution. However, the difference at high potential is negligible.

The voltammetric behaviour of the subsequent cycles with and without urea shows a decrease in the current density compared with the first cycle.

It should be noted that, just after the first cycle, higher currents are recorded in the potential 0.55–1.15 V range without urea compared to those found in the presence of urea. This behaviour suggests the formation of a slightly passivating polymeric film on the electrode surface, which depressed the anodic current by blocking the sites available for the oxygen evolution. However, further investigations on this point are necessary to draw definitive conclusions.

3.3 Pilot plant testing

Electrochemical oxidation of simulated humidity condensate was performed under galvanostatic conditions with the

equipment described in the experimental section. Two different types of anodes were employed: a commercial Pt/Ru on a DSA support and an SnO_2–Sb_2O_5 coating on a Ti electrode prepared in the laboratory. The tests were carried out until stable TOC values were reached.

The TOC profiles vs. electrolysis time on Pt/Ru anodes are reported in Fig. 5 for different current intensities. Initially the TOC level rapidly decreased due to the fast oxidation of the organics with the formation of intermediate species. The TOC values then tended to stabilize; it was observed that by reversing the cell polarity for 15 min (indicated by small arrows) a further TOC decrease could be obtained. The beneficial effect on SnO_2–Sb_2O_5 can be understood by taking into account the local pH changes that favour the restoration of highly oxidizing conditions, together with possible destruction of polymeric films on the anode surface; the higher current efficiencies of Pt/Ru could instead be related to the temporarily removal of the oxygen film blocking the anode active sites, during polarity inversion.

Figure 6 compares the TOC abatement for the two different anodes at a current intensity of 0.2 A; a remarkably better performance of the SnO_2–Sb_2O_5 electrode than the commercial one can be observed. In the case of tin dioxide electrodes, higher oxidation states are not available, therefore hydroxyl radicals react with the organic substances until complete oxidation to carbon dioxide and water. Strong adsorption of the organic substrate could hinder the generation of hydroxyl radicals on a non-active electrode surface, and limit the complete removal. On the other hand, when group VIII metals are used, as for the Pt/Ru anode, higher oxidation states for the metal ions are available, therefore the organic substances are partially decomposed by direct electrochemical oxidation.

The tests performed at high current intensities, as illustrated in Fig. 5, did not show any improvement in the organics removal. This could be related to the surface concentration of the OH radicals as a consequence of the competing reactions: organic substance oxidation and oxygen evolution [14].

This result can be explained by the weak interaction between the organic substances and the mixed oxide. Any further increase in the current density, would lead to higher oxygen evolution rates, rather than a more effective pollution oxidation. This is also justified by a greater pH drop at higher current density. A high evolution of oxygen leads to a lack of adsorption of the dissolved species with unfavourable kinetic conditions for the direct oxidation. The total current efficiency for the anodic oxidation during the process was calculated, using the following relationship:

$$\mathrm{TCE} = FVn\left(\frac{\left[(\mathrm{TOC})_i - (\mathrm{TOC})_f\right]}{12I\Delta T}\right)$$

where $(\mathrm{TOC})_i$ and $(\mathrm{TOC})_f$ are the total organic carbon (g L^{-1}) at the initial and final times, respectively; I is the current (A), F the Faraday constant (96487 C mol^{-1}), V the volume of the electrolyte (dm^3) and 12 is the molar mass of the carbon and n (9.93) is the number of electrons exchanged during the reaction. When the shuttle condensate water is simulated in the anolyte, several organic compounds with different oxidation numbers are present, therefore for a reliable evaluation of n it was necessary to compute the contribution of each compound to the concentration of the oxidized contaminants by carrying out a molar mass balance. The TCE values at a current intensity

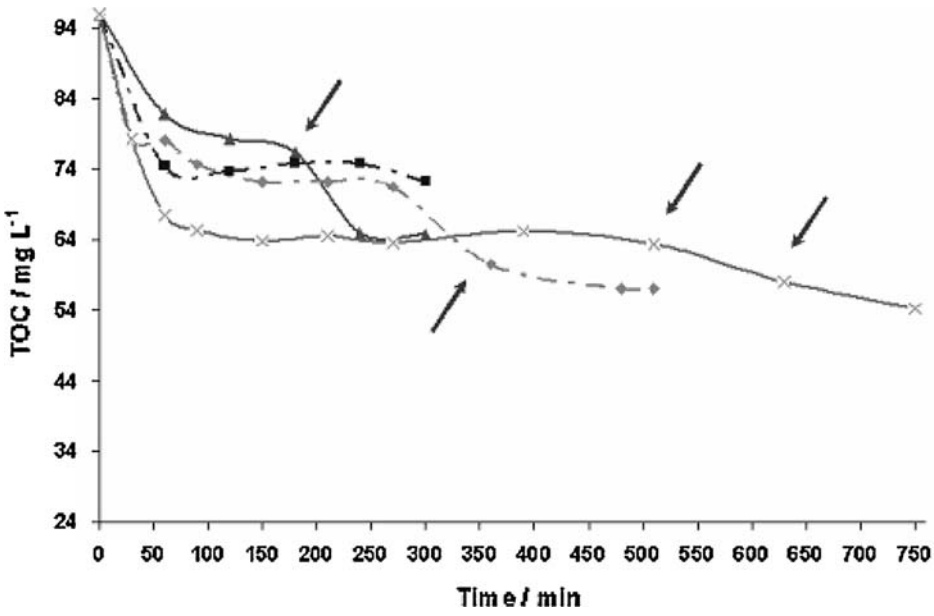

Fig. 5 TOC evolution versus time of the humidity condensates electro-oxidation test in divided cell using a cationic membrane with the Pt/Ru anode and stainless steel cathode at different current densities: 5–7 A (*filled square*); 2 A (*filled triangle*); 0.4A (*filled diamond*); 0.2–0.3 A (×). Electrolyte: Na_2SO_4 0.01 M

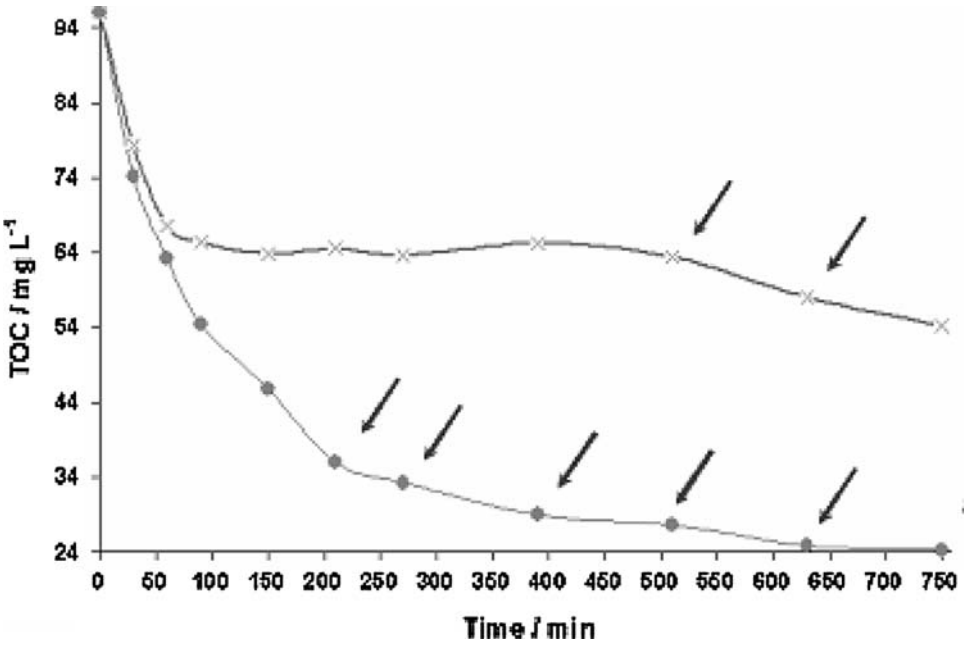

Fig. 6 Comparison of the TOC evolution vs. time between the Pt/Ru and SnO_2/Sb_2O_5 anodes in humidity condensates electro-oxidation test in divided cell at 0.2 A; Pt/Ru CM (×); SnO_2/Sb_2O_5 CM (*filled circle*). Electrolyte: Na_2SO_4 0.01 M

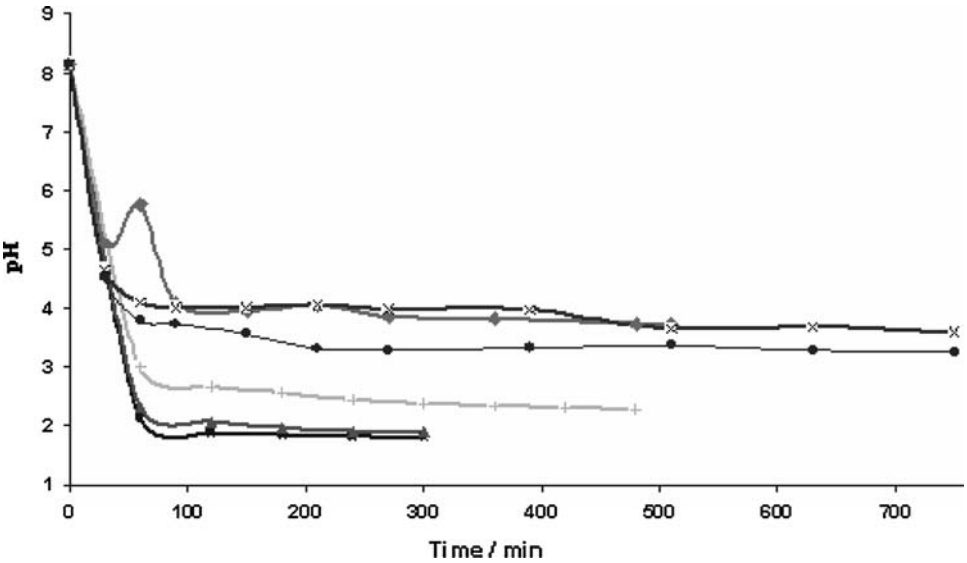

Fig. 7 Evolution of the pH vs. time during the electro-oxidation of humidity condensates in divided cell. Pt/Ru CM 5–7 A (*filled square*); Pt/Ru CM 2 A (*filled triangle*); Pt/Ru AM 0.8 A (+); Pt/Ru CM 0.4 A (*filled diamond*); Pt/Ru CM 0.2–0.3 A (×); SnO_2/Sb_2O_5 CM 0.2 A (*filled circle*). Electrolyte: Na_2SO_4 0.01 M

of 0.2 A for SnO_2–Sb_2O_5 and Pt/Ru are 25.62 and 14.94%, respectively.

These low values can be attributed to two different phenomena: (i) the complexity of the liquid matrix leads to a number of reaction intermediates; (ii) the intensive adsorption of the dissolved species on the electrode surface blocks the active sites.

Figure 7 shows the change in pH during the tests. At the beginning, a sharp pH decrease was observed then, after about 1 h, the pH remained almost constant. This dramatic pH decrease was probably due to different effects: the formation of organic acids as intermediates in the electro-oxidation and acidification as a consequence of the O_2 evolution with the formation of H^+, which was partly unbalanced due to the simultaneous transfer of the protons and other cations (particularly NH_4^+) through the cationic membrane to compensate for the applied current intensity. By increasing the current intensity, the pH drop resulted to be higher due to the increase in the oxygen evolution.

During the tests, concentration changes in the nitrogen species versus time were observed, as illustrated in Figs. 8 and 9. Nitrogen mass balance in the humidity condensate shows a value of about 28 mg L^{-1} (expressed as ammonia), mainly due to NH_4HCO_3 and NH_4NO_3, and nitrogen organic substances as caprolactam and urea; whereas nitrate and/or nitrite were almost absent. The ammonium ions, subjected to electro-migration and diffusion, were able to move through the cationic membrane from the

anodic to the cathodic compartment, where the basic environment converted them into ammonia. In fact, the measured ammonia concentration in the cathodic compartment increased in time up to a value of about 23 mg L^{-1}.

This is in agreement with the marked decrease in the ammonium ions observed in the first hour of treatment, see Fig. 8. For the tests carried out at higher current intensity, a noticeable increase in the NO_3^- concentration was initially noted up to a rather stable value (see Fig. 9). This can be explained in terms of possible direct oxidation of the ammonia species (also those coming from the oxidation of the organics) on the anode surface, due to the high anodic potential.

Several tests performed with an anionic membrane that hindered the cations flow provided quite different results. The data in Fig. 8 show that a marked decrease in the ammonia species was not observed. During the tests, an oscillating behaviour was found for the ammonia species concentration, probably due to the competition between the formation of ammonia by oxidation of the organic compounds and partial conversion of this ammonia species into nitrates (see Fig. 9). This behaviour is also closely connected to the nature and concentration of organic pollutants.

It can be seen from the nitrogen mass balance carried out at the end of the test, that only small amounts of nitrogen are formed, unlike for direct oxidation at the electrode surface, where nitrogen organic compounds are subjected to complete mineralization to CO_2 and water [31]. In fact, the oxidation mechanism depends both on the nature of the molecule and on the properties of the electrode surface, according to different mechanisms, which lead to variable amounts of nitrates or ammonium ions.

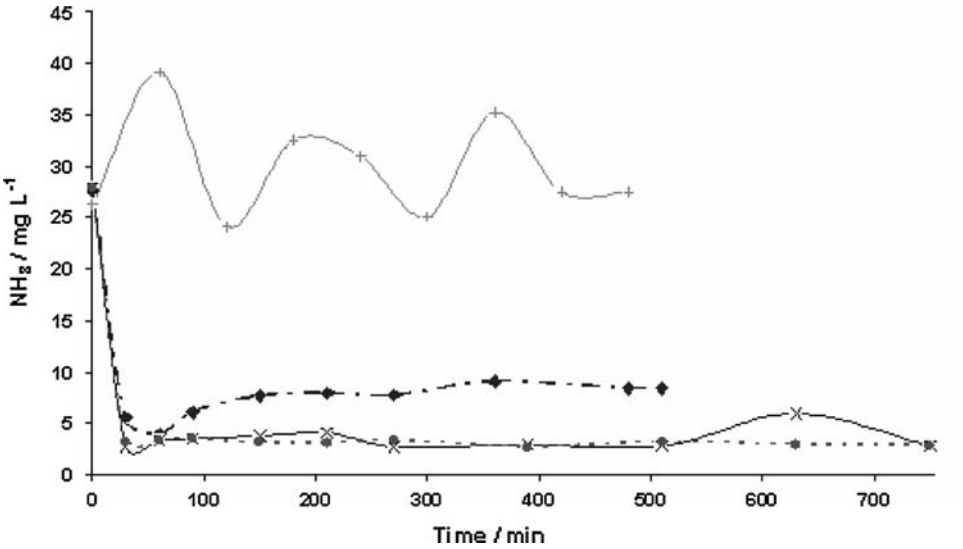

Fig. 8 NH_3 evolution vs. time during the electro-oxidation of humidity condensates in divided cell. Pt/Ru AM 0.8 A (+); Pt/Ru CM 0.4 A (*filled diamond*); Pt/Ru CM 0.2–0.3 A (×); SnO_2/Sb_2O_5 CM 0.2 A (*filled circle*). Electrolyte: Na_2SO_4 0.01 M

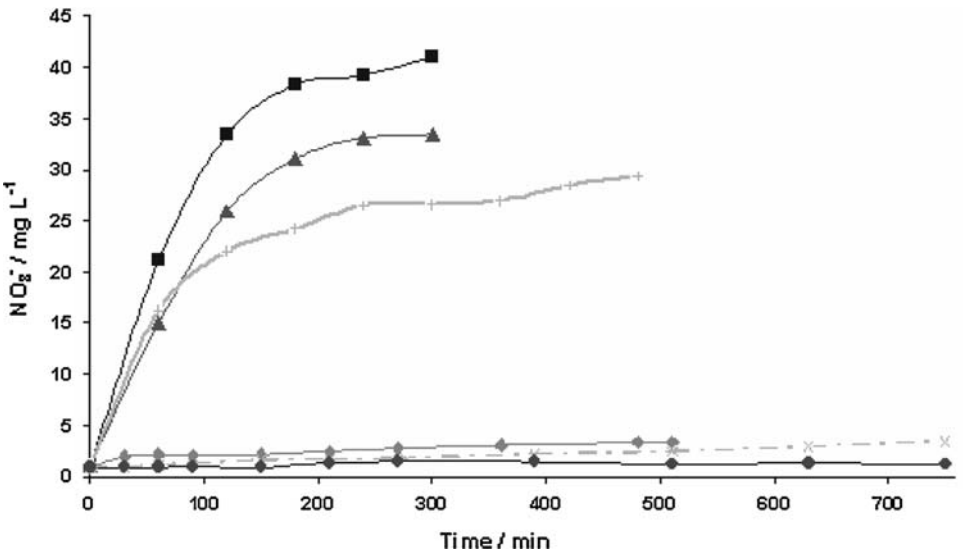

Fig. 9 NO_3^- evolution vs. time during the electro-oxidation of humidity condensates in divided cell. Pt/Ru CM 5–7 A (*filled square*); Pt/Ru CM 2 A (*filled triangle*); Pt/Ru AM 0.8A (+); Pt/Ru CM 0.4 A (*filled diamond*); Pt/Ru CM 0.2–0.3 A (×); SnO_2/Sb_2O_5 CM 0.2 A (*filled circle*). Electrolyte: Na_2SO_4 0.01 M

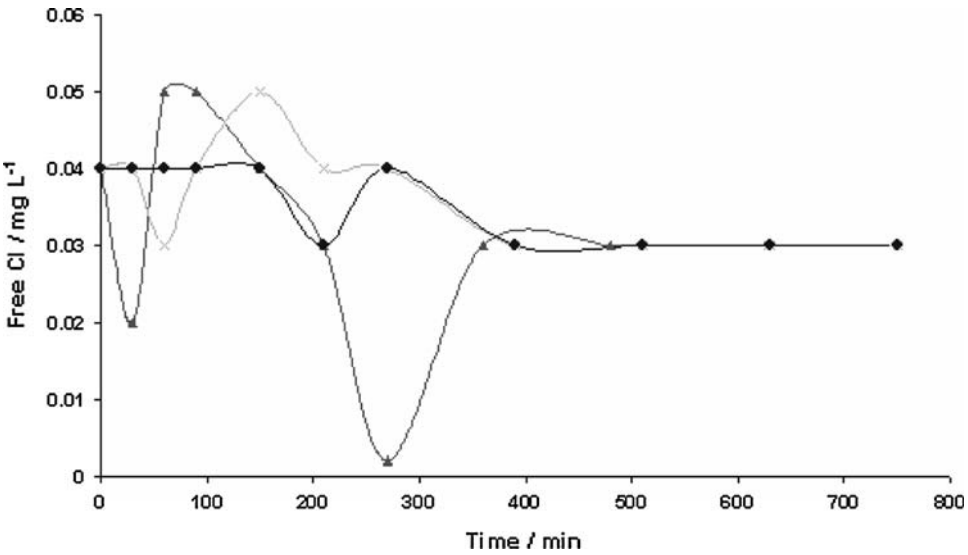

Fig. 10 Free Cl evolution vs. time during the electro-oxidation of humidity condensates in divided cell. Pt/Ru CM 0.4 A (*filled triangle*); Pt/Ru CM 0.2–0.3 A (×); SnO_2/Sb_2O_5 CM 0.2 A (*filled circle*). Electrolyte: Na_2SO_4 0.01 M

This is related to the presence or absence of a hydrogen atom linked to the carbon of the carboxylic group. Urea and caprolactam, two of the contaminants with higher concentrations in the humidity condensate, produce a three times higher amount of nitrate than that of ammonium.

Figure 10 shows the trend with time of the free chlorine concentration, which after an initial transient of about 6 h, reached a quite constant concentration of 30 ppb, corresponding to the presence of dissolved chlorides.

The total chlorine amount was almost constant in time in each tests, while the changes of free chlorine concentration were probably due to the formation of chloro-amines, with a consequent increase in the combined chlorine concentration.

One possible mechanism could be due to the reaction of chlorine in the anodic compartment as follows:

$$2Cl^- \rightarrow Cl_2 + 2e^-(aq) \quad (1)$$

where, under slightly acidic conditions, the following reaction is favoured:

$$Cl_2 + H_2O \rightarrow HClO + H^+ + Cl^- \quad (2)$$

forming hypochlorous acid, which, being a strong oxidant, can easily react with many organic species, thus regenerating chloride ions:

$$HClO(aq) + H^+ + 2e^- \rightarrow Cl^- + H_2O \quad (3)$$

which can continue the cycle.

Urea was used as a test molecule to understand the reaction mechanisms of the organic substances degradation and the influence of the combined direct and indirect electro-oxidation. The experiments were performed at different current densities using a divided cell with a Pt/Ru anode and a cationic membrane; urea concentration of 2 g L^{-1} was used, in a supporting electrolyte consisting of 0.01 M sodium sulphate and 0.05 M sodium chloride.

Figure 11 (B graph) shows that the formation of nitrates follows an exponential profile with electrolysis time. The process is mainly due to direct electro-oxidation on the active surface of electrodes, which mainly depends on urea adsorption.

Under these conditions, a limited recovery of ammonia quantities is obtained in the urea oxidation process, thus confirming a reaction mechanism that produces higher quantities of nitrates. Furthermore, in the bulk solution, the ammonium ions can react with hypochlorous acid, according to the following reaction:

$$2NH_4^+ + 3HClO \rightarrow N_2 + 3H_2O + 5H^+ + 3Cl^- \quad (4)$$

and thus further reduce the ammonia concentration in the anodic solution.

At much higher current densities (from 30 to 200 A m^{-2}), neither the increase in nitrate formation nor the increase in the recovered ammonia in the cathodic compartment were found to follow the expected increase in the current density. These results show, once again, that when the current density is increased to a great extent only a remarkably higher oxygen evolution is observed. It was also found that urea, in an acid environment, reacts with hypochlorous acid anion according to a homogeneous multi-step process:

$$NH_2CONH_2 + 3OCl^- \rightarrow N_2 + CO_2 + 3Cl^- + 2H_2O \quad (5)$$

forming nitrogen and carbon dioxide. In Fig. 11 (A graph) the amount of chloramines is quite low, except for the test at 30 A m^{-2}, where it reaches a maximum value and then decreases due to indirect electro-oxidation in the bulk solution.

The increase in sodium chloride concentration not only led to higher levels of chloramines but did not practically change the contaminant removal efficiency, because the limiting factor is the active chlorine concentration in the

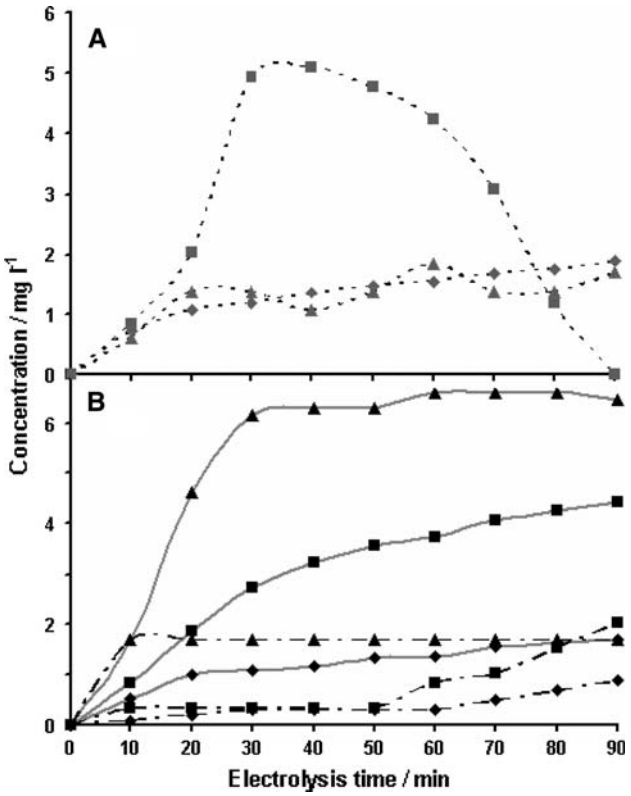

Fig. 11 By-products evolution vs. time during the electro-oxidation of urea (2 g L^{-1}) over a Pt/Ru at different current density. Electrolyte: Na_2SO_4 0.01 M + NaCl 0.05 M. **A** Chloramines. **B** Nitrates (continuous line) and ammonia in the cathodic chamber (dashed line). Legend: 0.5 A m^{-2} (*filled diamond*); 30 A m^{-2} (*filled square*); 200 A m^{-2} (*filled triangle*)

solution, which, in turn, depends on direct electro-oxidation of the chloride ions on the anodic electrode surface.

4 Conclusions

TOC concentration abatement was monitored via electro-oxidation tests. The best removal of organic compounds was obtained using a suitably synthesized SnO_2/Sb_2O_5 electrode with 24 depositions. The preparation of the Ti support was particularly important to provide an optimal adhesion between the catalytic layer and the electrode support, thus assuring a longer stability and life time of the anode.

Higher removal efficiencies were obtained with the SnO_2/Sb_2O_5 electrode due to its better catalytic activity, than that of commercial electrodes, but also because of connection to the larger anode surface available for the pollutant oxidation. The inversion of the electrode polarity seemed to offer a further advantage as far as the TOC removal in the contaminant solution is concerned.

The removal efficiency in the electro-oxidation test appeared to be depressed for both electrodes at high current density. In these conditions, when non-active anodes such as SnO_2/Sb_2O_5 are used, the removal efficiency mainly depends on the capacity to generate OH radicals, which in turn is limited by the adsorption of organic compounds on the electrode surface. For active Pt/Ru anodes, the removal efficiency mainly depends on the degree of adsorption of the organic substances, which can be limited by the rate of oxygen evolution that inhibits the adsorption sites for organic compounds. Confirmation of this interpretation was provided from the tests carried out in the presence of urea at a high current density, which showed the formation of lower nitrate species than expected. The formation of nitrate species is in fact clear evidence of direct electro-oxidation.

As future work, SnO_2 electrodes on Ti with several Sb concentrations will be prepared, in order to study their electrochemical performance. According to the NASA protocol, tests must be carried out introducing all possible contaminants into the distillate water. These studies allowed us to determine the global efficiency of the process, while tests on the individual pollutants will help us to recognize all the reaction intermediates.

Electrodes prepared via sputtering and chemical vapour deposition will also be tested.

Acknowledgments The Regione Piemonte Research Project "Water Monitoring and Regeneration during Space Missions" financial support is gratefully acknowledged.

References

1. Behrend AF Jr, MacElroy RD, Reysa RP (1991) Regenerative life support systems & processes, SP-873, SAE International
2. Griffin MR, Backsay AM (1991) Space station ECLSS and thermal control, SP-875, SAE International
3. Atwater JE (1995) J Environ Sci Health A30 (4):817–830
4. Carter DL, Holder DW, Alexandre K, Shaw RG, Hayase JK (1991) Preliminary ECLSS waste water, 21st international conference on environmental systems, SAE 951150
5. Carter DL, Cole H, Habercom M, Griffith G, Slivon L (1992) Determination of organic carbon and ionic accountability of various waste and product water derived from ECLSS water recovery tests and spacelab humidity condensate, 22nd international conference on environmental systems, SAE 921313
6. Carter DL, Bagdigian RM (1993) Phase III integrated water recovery testing at MSFC: single loop test results and lessons learned water, 23rd international conference on environmental systems, SAE 932048
7. Sauer RL, Pierre LM, Schultz JR, Sinyak YE, Skuratov VM, Protasov NN, Bobe LS (1999) Chemical analysis of potable water and humidity condensate: phase one and lessons learned, 29th international conference on environmental systems, SAE 1999-01-2028
8. Akse JR, Holtsnider JT, Carter L (2004) Mesoporous oxide supported catalysts for low temperature oxidation of dissolved organics in spacecraft wastewater streams, 34th international conference on environmental systems, SAE 2004-01-2405
9. Putnam DF, Vaughan RL (1971) Water reclamation from urine by electrolysis-electrodialysis. American Society of Mechanical

Engineers, Society of Automotive Engineers, and American Institute of Aeronautics and Astronautics, Life support and environmental control conference, San Francisco, CA, July 12–14, 1971. New York, American Society of Mechanical Engineers. ASME PAPER 71-AV-11
10. Akse JR, Atwater JE, Shussel LJ, Thompson JO, Verostko CE (1993) Development and fabrication of a breadboard electrochemical water recovery system, 23rd international conference on environmental systems, SAE 932032
11. Mitchell KL (1993) Technical assessment of Mir-1 life support hardware for the international space station, life support systems Branch/ED62. George C. Marshall Space Flight Center, Huntsville, Alabama
12. Akse JR, Atwater JE, Jolly C, Thompson JO, Wheeler RR Jr (1994) A breadboard electrochemical water recovery system for producing potable water from composite wastewater generated in enclosed habitats, electrochemical society symposium on water purification by photocatalytic, photoelectrochemical and electrochemical processes
13. Comninellis C (1994) Electrochim Acta 39:1857–1862
14. Comninellis C, De Battisti A (1996) J Chim Phys 93:673–679
15. Winograd N (1984) Laboratory techniques in electroanalytical chemistry. In: Kissinger PT, Heineman WR (eds) Marcel Dekker, New York
16. Jarzebsky ZM, Marton JP (1976) J Electrochem Soc 123:299C–310C
17. Meaney KL, Omanovic S (2007) Mater Chem Phys 105:143–147
18. Duverneuil P, Maury F, Pebere N, Senocq F, Vergnes H (2002) Surf Coat Technol 151–152:9–13
19. Hy D, Feng YJ, Liu JF (2007) Mater Lett 61:4920–4923
20. Correa-Lozano B, Comninellis C, De Battisti A (1996) J Electrochem Soc. 143:203–209
21. Yao P, Chen X, Wu H, Wang D (2008) Surf Coat Technol (in press) doi:10.1016/j.surfcoat.2008.01.026
22. De Pauli CP, Trasatti S (1995) J Electranal Chem 396:161–168
23. Alves VA, Da Silva LA, Boodts JFC, Transatti S (1994) Electrochim Acta 39:1585–1589
24. Onuchukwa AI, Transatti S (1991) J Appl Electrochem 21:858–862
25. Vercesi GP, Rolewicz J, Comninellis C (1991) Thermochim Acta 176:31–47
26. Lipp L, Pletcher D (1997) Electrochim Acta 42:1091–1099
27. Lide DR (1995) CRC handbook of physics and chemistry, 76th edn., CRC Press, Boca Roton
28. Lassali TAF, Boodts JFC, Bulhoes LOS (2000) J Appl Electrochem 30:625–634
29. Montilla F, Morallòn E, De Battisti A, Vazquez JL (2004) J Phys Chem B108:5036–5043
30. Kotz R, Stucki S, Carcer B (1991) J Appl Electrochem 21:14–20
31. Simka W, Piotrowsky J, Nawrat G (2007) Electrochim Acta 52:5696–5703